NPS ARCHIVE
1967
CLAUSNER, E.

CHARACTERISTIC FEATURES OF THE FLORIDA CURRENT

EDWARD CLAUSNER, JR.

LIBRARY
NAVAL POSTGRADUATE SCHOOL
MONTEREY, CALIF. 93940

THE UNIVERSITY OF MIAMI

CHARACTERISTIC FEATURES OF THE FLORIDA CURRENT

BY

Edward Clausner, Jr.

A THESIS

Submitted to the Faculty
of the University of Miami
in partial fulfillment of the requirements for
the degree of Master of Science

Coral Gables, Florida

May, 1967

NPS ARCHIVE
1967
CLAUSNER, E.

LIBRARY
NAVAL POSTGRADUATE SCHOOL
MONTEREY, CALIF. 93940

THE UNIVERSITY OF MIAMI

A thesis submitted in partial fulfillment of
the requirements for the degree of
Master of Science

Subject

Characteristic Features of the Florida Current

Edward Clausner, Jr.

ABSTRACT

Characteristic features of the velocity and temperature fields in the Florida Current are isolated and discussed on the basis of time-averaged free instrument data obtained during approximately 40 transects across the current at four separate sections during 1965-1966. The sections, from Marathon - Cay Sal Bank to Ft. Pierce - Matanilla Shoal, encompass a 225 km downstream distance within the Florida Straits.

The dominant feature isolated is a downstream acceleration of the subsurface current, associated with the convergent downstream cross-sectional area of the Straits. A uniaxial surface current and the cross-stream component of the subsurface current are also intimately linked with the convergence and divergence of the cross-channel width. The mass field adjusts to changes in current velocity as would be anticipated from Bernoulli's Equation. Comparison of the results of the free instrument technique with previous time-averaged data taken in this area shows close agreement.

ACKNOWLEDGEMENTS

This is the first report of the results of data obtained by the free instrument technique encompassing two years of experiments in the Florida Straits. However, it is due to the kindness and interest of Dr. William S. Richardson, Professor of Oceanography, and his associates that I was permitted to utilize the total data and to assist in the planning and execution of a small portion of this work. I am particularly indebted to Dr. William J. Schmitz, Jr., for showing me the fine structure of scientific research and for changing my fathoms to meters, my knots to cm/sec, and my spin to vorticity.

I also want to thank the rest of the Southeastern Massachusetts Technological Society; Fred White, who has forgotten more about boats than I ever knew, and Angelo Cangiamila, who made the blueprints come to life. In addition, I would like to express my appreciation to Fred Koch for assisting in the computer programming, and to the young ladies who punched innumerable IBM cards and typed the many drafts of this thesis; Ann Calvert, Elaine Hallett, Ann Dolney, and Carla Cangiamila.

Many thanks are also in order for the members of my thesis committee for their constructive guidance in the preparation of this thesis: Dr. William S. Richardson, Dr. William J. Schmitz, Jr., Dr. Leonard J. Greenfield, Dr. Eugene F. Corcoran, Dr. Russel L. Synder, Dr. Edwin S. Iverson, and Dr. Saul Broida.

Finally, I wish to convey my gratitude and respect to my

running-mate, LT Edward J. O'Brien,III, USN, whose moral, mental, and physical support during the last two years was invaluable.

Support for this work was provided by the Office of Naval Research.

CDR Edward Clausner, Jr., USN

Coral Gables, Florida
May, 1967

TABLE OF CONTENTS

Page

LIST OF TABLES..... vii

LIST OF FIGURES.....viii

I. INTRODUCTION..... 1

II. THE EXPERIMENT..... 5

A. Method..... 5

B. Sampling Requirements..... 5

C. Field Program..... 11

D. Data Analysis..... 11

E. Errors..... 14

III. RESULTS..... 16

A. Discussion..... 16

B. Comparison with Other Methods..... 40

IV. SUMMARY..... 52

LITERATURE CITED..... 54

LIST OF TABLES

TABLE		Page
I.	The Field Program	12
II.	Positioning Constants	13
III.	Basic Data for Section I	17
IV.	Basic Data for Section II	18
V.	Basic Data for Section III	19
VI.	Basic Data for Section IV	20

LIST OF FIGURES

FIGURE		Page
1.	Section Locations	3
2.	Station Location and Drop Spacing for Sections I and II	7
3.	Station Location and Drop Spacing for Sections III and IV	9
4.	Downstream Surface Current (V_s) vs Cross-Stream Distance for Sections I and II	21
5.	Downstream Surface Current (V_s) vs Cross-Stream Distance for Sections III and IV	23
6.	Smoothed Downstream (V) Isotachs for Sections I and II	25
7.	Smoothed Downstream (V) Isotachs for Sections III and IV	27
8.	Smoothed Cross-Stream (U) Isotachs for Sections I and II	29
9.	Smoothed Cross-Stream (U) Isotachs for Sections III and IV	31
10.	Isotherm Depths for Sections I and II	33
11.	Isotherm Depths for Sections III and IV	35
12.	Comparison of Free Instrument Surface and Subsurface Current Data at Section II with Current Meter Data	41
13.	Comparison of Free Instrument Surface Current Data at Sections I and II with GEK Data	44
14.	Comparison of Free Instrument Mass Field Data at Sections I and IV with Hydrographic Data	48
15.	Comparison of Free Instrument Mass Field Data at Section II with Time-Averaged Hydrographic Data	50

I. INTRODUCTION

The purpose of this thesis is to isolate and discuss certain characteristic features of the Florida Current on the basis of data obtained by direct measurement using the free instrument method (Richardson and Schmitz, 1965). From six to twelve transects were made along each of four sections across the current encompassing a 225 km downstream distance within the Florida Straits (Figure 1). Within this segment of the Florida Current, the surface and subsurface structure and isotherm distribution will be presented and discussed with particular emphasis on their adjustment to the changing downstream geometry of the Florida Straits. The data has been time-averaged to keep tidal influences to a minimum in approximating steady state conditions, and is the first detailed description of the results of free instrument measurements.

Although there is extensive literature on the Florida Current, this paper represents a considerable addition to the previous work done in this area. Undoubtedly, the most thorough investigation of the Florida Current by any method was made by Pillsbury (1890). However, the majority of information obtained in the past has been made by indirect methods, such as the GEK (geomagnetic electrokinetograph) and geostrophic interpretations based on hydrographic data. In addition, due to the nature of the current fluctuations, previous attempts to approximate steady state conditions have been biased in inverse proportion to the time and number of samples taken.

A comparison will be made between the results of the free instrument method and results obtained by current meter measurement (Pillsbury, 1890), the GEK (Webster, 1961), (Murray, 1952) and (Chew and Wagner, 1956), and hydrographic data (Chew and Wagner, 1956), (Worthington, 1966) and (Broida, 1962a, 1962b, 1963 and 1964).

The technique used to obtain the data in this thesis will be referred to as the "free instrument method", and yields a direct measurement of the vertically averaged current over a water column. Preliminary evaluation of the free instrument technique and its applicability to the Florida Current was conducted in 1964 (Richardson and Schmitz, 1965). This pilot data clearly indicated the existence of well defined features of the mass and velocity fields of the Florida Current. Based on this pilot data, a series of experiments were devised and conducted in 1965-1966 in order to observe both the cross-stream distribution and downstream changes of mass and current field structure over the greater portion of the Florida Current.

Figure 1. Section Locations

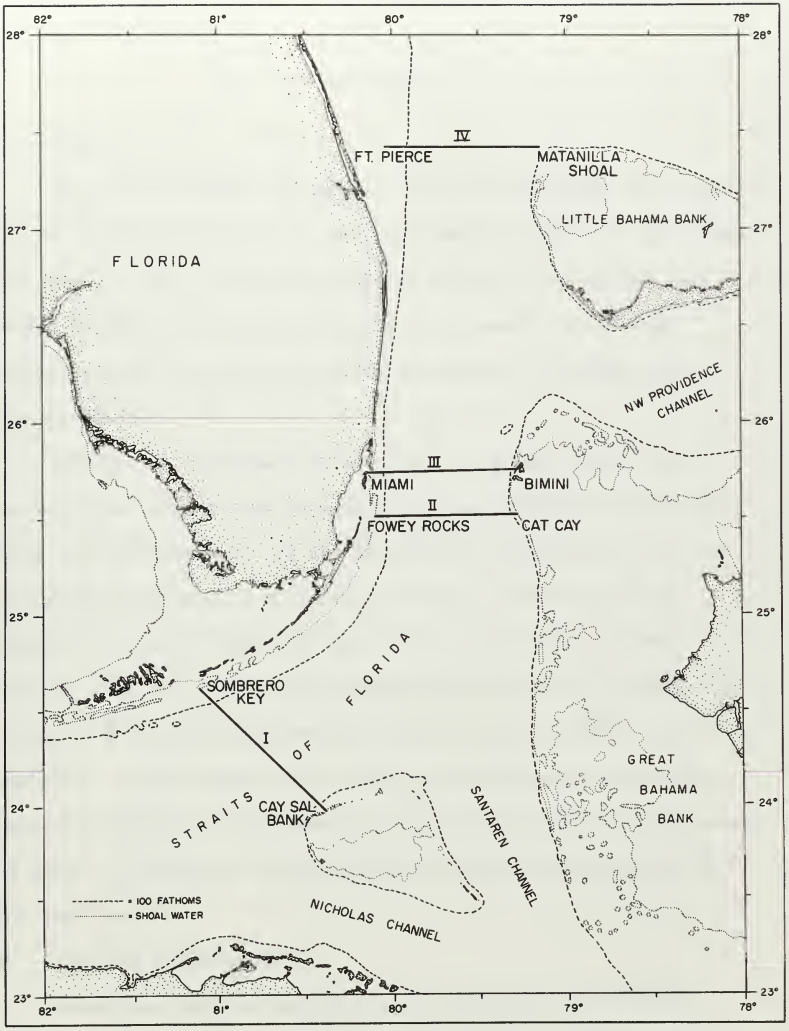
82°
81°
80°
79°
78°
28°
27°
26°
25°
24°
23°
IV
FT. PIERCE
MATANILLA SHOAL
LITTLE BAHAMA BANK
FLORIDA
NW PROVIDENCE CHANNEL
III
MIAMI
BIMINI
II
FOWEY ROCKS
CAT CAY
SOMBRERO KEY
I
STRAITS OF FLORIDA
GREAT BAHAMA BANK
CAY SAL BANK
SANTAREN CHANNEL
NICHOLAS CHANNEL
100 FATHOMS
SHOAL WATER

II. THE EXPERIMENT

A. Method

The free instrument technique yields the magnitude and direction of the vertically averaged current and the transport per unit width of a water column from measurements of run time, depth, and horizontal deflection of a freely falling instrument. A thorough description of this method has been presented by Richardson and Schmitz (1965).

Briefly, an instrument falls freely to a preselected depth, where ballast weights are released, and then returns to the surface under its own buoyancy. If the horizontal displacement ($\vec{X}$) of the instrument from drop to surfacing is known, together with the elapsed run time (t) and the depth (h) to which the instrument travels, then the vertically averaged velocity over the depth of flight is $\frac{\vec{X}}{t}$ and the transport per unit width to h is $\frac{\vec{X}h}{t}$. In addition, a 16mm camera housed within the instrument takes time-lapse photographs of a thermometer and pressure gauge at about every 20 meters of depth, yielding a vertical temperature distribution for each drop.

B. Sampling Requirements

Downstream section spacing between Sections I and IV was dictated by a desire to observe the Florida Current over varying topography and cross-sectional area on the maximum downstream scale possible within the confines of the Florida Straits and the

limitations imposed by the political situation to the South. The location of Sections II and III was chosen in order to study a convergent sector of the channel in isolation.

Cross-stream station spacing was determined by the results of pilot data and previous work in the Florida Current. Station spacing of 10 km in the anticyclonic zone was considered adequate and a 5 km spacing was used in the cyclonic zone since cross-stream variations in this region are about twice those in the anticyclonic zone. Abrupt shear zones of 3-5 km were expected on both edges of the channel.

Vertical sampling consisted of dropping one to six instruments at each station in each cross-section, depending upon depth. One bottom drop was made at each station. In Sections II and III, instruments were dropped to the expected depth of the layers of vertically averaged sigma-t of 25 and 26. In Sections I and IV, instruments were more closely spaced and dropped to standard depths in order to obtain a more detailed picture of the velocity structure of the current. Station and drop spacing for each Section is shown in Figures 2 and 3.

Time sampling was determined by the speed of the research vessel, the limitation of being able to operate only in the daytime, and the requirements for random sampling over periods of significant fluctuations of the mean current. Based on pilot data accumulated over a nine-month period in 1964-65, the dominant time variations appeared to be of tidal character. Therefore, an attempt was made to minimize rectification from tidal time scales. The previous method of sampling each station on every transect was abandoned in Sections I

Figure 2. Station Location and
Drop Spacing - Sections I and II.

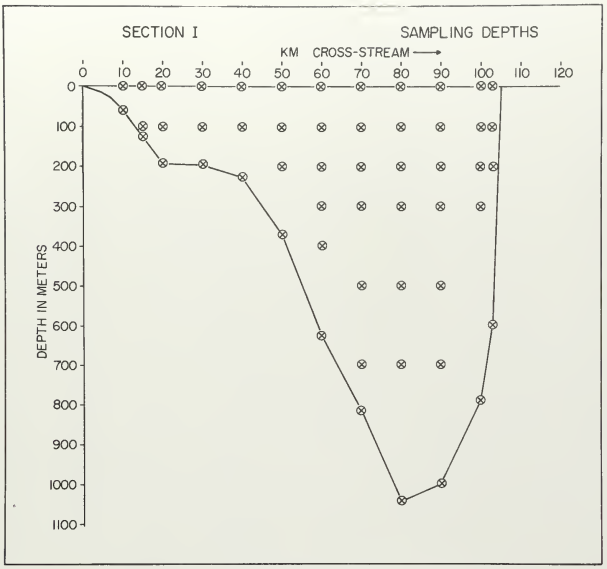
SECTION I
SAMPLING DEPTHS
KM CROSS-STREAM →
0 10 20 30 40 50 60 70 80 90 100 110 120
DEPTH IN METERS
0 100 200 300 400 500 600 700 800 900 1000 1100

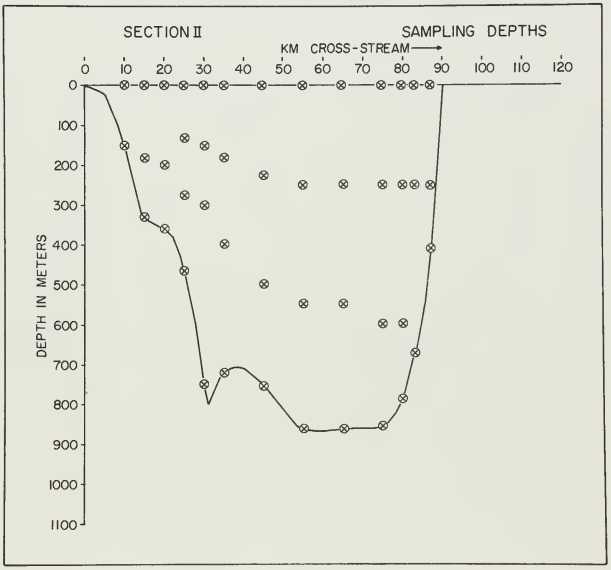
SECTION II
SAMPLING DEPTHS
KM CROSS-STREAM →
0 10 20 30 40 50 60 70 80 90 100 110 120
DEPTH IN METERS
0 100 200 300 400 500 600 700 800 900 1000 1100

Figure 3. Station Location and
Drop Spacing - Sections III and IV.

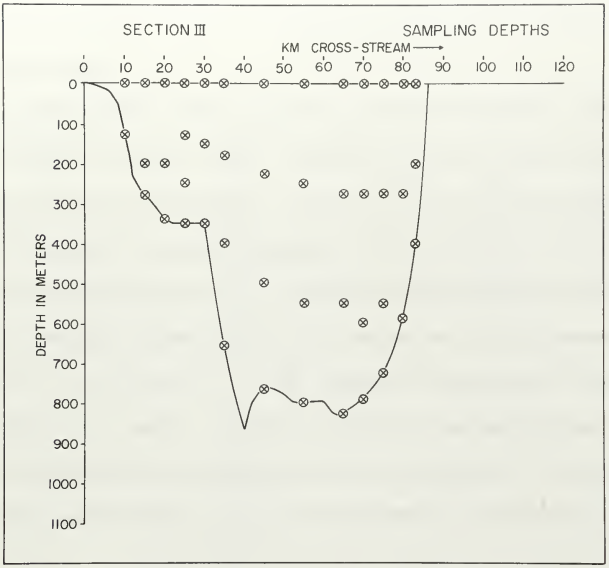
SECTION III
SAMPLING DEPTHS
KM CROSS-STREAM
0 10 20 30 40 50 60 70 80 90 100 110 120
DEPTH IN METERS
0 100 200 300 400 500 600 700 800 900 1000 1100

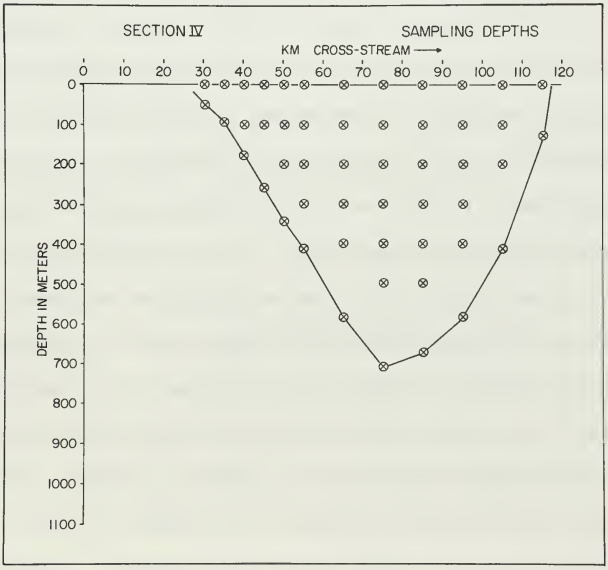
SECTION IV
SAMPLING DEPTHS
KM CROSS-STREAM
0 10 20 30 40 50 60 70 80 90 100 110 120
DEPTH IN METERS
0 100 200 300 400 500 600 700 800 900 1000 1100

and IV due to the speed and handling limitations of R/V AUSTAUSCH.

C. Field Program

Observations were made along two sections completed in 1965; Miami, Florida to Bimini, B.W.I. (Section III), and from just south of Fowey Rocks to Cat Cay, B.W.I. (Section II), and two sections completed during the period June-August 1966; Marathon (Vaca Key), Florida to Cay Sal Bank, B.W.I. (Section I), and from Ft. Pierce, Florida to Matanilla Shoal on the N.W. corner of Little Bahama Bank (Section IV), see Figure 1. It was planned to sample each section over a period of a month. However, Section I was interrupted for a week due to bad weather and Section IV was terminated 13 days early due to structural failure on the R/V AUSTAUSCH, (see Tables I and II).

D. Data Analysis

Depth as a function of time for each run is plotted and extrapolated slightly at the drop and surfacing points as well as the bottom of the run in order to obtain both run time and run depth. Surface current is computed from three fixes taken on a surface buoy. The surfacing position of each instrument is then extrapolated back from its recovery position. The average velocity and transport per unit width are calculated for each run, and are then plotted against depth on a station basis and time-averaged by curve fitting. The distribution of transport per unit width is differentiated for the velocity distribution, which is then plotted on a station basis. The same basic sequence is followed for temperature-depth for each run, i.e., plotted on a station basis and time-averaged by curve fitting. A section plot is then made of six selected isotherms

TABLE I

FIELD PROGRAM

Section	Inclusive Dates	Number of Stations	Average Number of Times Each Station Sampled	Total Usable Instrument Drops Each Section
I	13 June - 4 July 1966	12	9	259
II	24 May - 24 June 1965	13	12	368
III	24 May - 24 June 1965	13	12	364
IV	26 July - 13 August 1966	12	6	177

TABLE II

POSITION CONSTANTS

Section		I	II	III	IV
Hi-Fix Slave Location	S 1	Collier Bldg. IMS, Virginia Key	Bahia Mar Marina, Ft. Lauderdale	Bahia Mar Marina, Ft. Lauderdale	Navy Pier, Port Canaveral
	S 2	City Pier, Marathon	Collier Bldg. IMS, Virginia Key	Collier Bldg. IMS, Virginia Key	Kiwi Motel, Ft. Pierce
S 1 Latitude (N)		25° 44.5'	25° 44.5'	25° 44.5'	27° 28.0'
S 1 Longitude (W)		80° 08.8'	80° 08.8'	80° 08.8'	80° 18.1'
S 2 Latitude (N)		24° 42.3'	26° 06.5'	26° 06.5'	28° 24.7'
S 2 Longitude (W)		81° 06.5'	80° 06.4'	80° 06.4'	80° 36.4'
Base Line: Orientation		039.5°T	007.1°T	007.1°T	344.0°T
Base Line: Length		148.5 km	42.6 km	42.6 km	109.4 km
Section: Orientation		317°T	270°T	270°T	270°T
Section: Width		100 km	85 km	80 km	85 km
Cartesian Coordinates	X	5-105 km	5-90 km	6-86 km	30-115 km
	Y	-6 km	-25 km	0 km	-5 km

Note: The origin of the cartesian coordinate systems are always at S 2.

and smoothed. The velocity components at the smoothed isotherm depths are read off the station plots and smoothed. The smoothing was used in order to obtain the most reasonable possible representation of the mean mass and current fields. These data are then listed for each of the six selected isotherms at up to fifteen cross-stream points (at each station and at the boundaries) for each section (see Tables III-VI). This format was chosen for ease in handling and presentation and because it is convenient for the testing of three-dimensional models of inertial currents in x,y,T (cross-stream, downstream, temperature) coordinates (Robinson, 1965).

E. Errors

Errors may be introduced from three sources: (1) interpretative errors associated with the assumption of steady state conditions over the time and space scales of a run, (2) instrument and computational errors, and (3) errors due to rectification in time-averaging.

Based on previous experience in the Florida Straits, interpretive errors due to fluctuations over the time and space scales of an instrument run are very small (1-3%) and measurements are to be considered as desirable averages (Richardson and Schmitz, 1965).

System errors in a single measurement of vertically averaged current (or transport per unit width) and isotherm depths are in the 3-10% range (Schmitz, 1966). Station locations are known to about 100 m or better. Subsurface current profiles obtained by differentiation of the transport profile are smoothed on both a station and section basis in order to minimize random system errors. Errors associated with obtaining a representation of the mean stream

using this technique are thought to be bounded by 5-10%. Individual errors are assumed to combine in a random manner yielding characteristic errors in time-averaged currents and isotherm depths of 3-5%.

Rectification errors in time-averaged downstream current speed and isotherm depth are estimated to about 3%. However, errors in cross-stream speeds due to this source may reach 25% (Schmitz and Richardson, 1966).

III. RESULTS

The basic data from this experiment are presented in Tables III-VI, and in Figures 4-11. These tables list cross-stream distance, time-averaged values of isotherm depth, downstream current speeds, and cross-stream speeds at six selected isotherms at up to fifteen points along each cross-section. Figures 4 and 5 give the downstream surface current component as a function of cross-stream distance with an envelope of maximum observed variations from time-averaged values. The remaining graphs are (for each section) downstream current component contours (Figures 6 and 7), cross-stream current component contours (Figures 8 and 9), and isotherm depths (Figures 10 and 11).

A. Discussion

(1) Topography. The topography of the Florida Straits is discussed in this thesis as it is cogent to downstream changes of velocity and mass field structure of the Florida Current. Furthermore, the navigational and depth accuracy of the instruments used make this description a meaningful addition to the topographical knowledge of this area.

In general, the cross-sectional area of the Straits decreases downstream. Cross-sectional areas are approximately 60 km^2 at Section I, 55 km^2 at Section II, 48 km^2 at Section III, and 36 km^2 at Section IV. There is a reduction in channel width at the surface as the cross-sectional area decreases downstream with the exception of Section IV, where the width at the surface diverges slightly

TABLE III - BASIC DATA FOR SECTION I

TABLE	Grid # → / Isotherms ↓	1	2	3	4	5	6	7	8	9	10	11	12	13	14	15
	26	*	10	15	20	30	40	50	60	70	80	90	100	103	105	**
	22	6	10	15	20	30	40	50	60	70	80	90	100	103	104	**
X	18	**	13	15	20	30	40	50	60	70	80	90	100	103	104	**
	14	**	**	18	20	30	40	50	60	70	80	90	100	103	104	**
	10	**	**	**	**	**	**	51	60	70	80	90	100	102	**	**
	8	**	**	**	**	**	**	57	60	70	80	90	100	**	**	**
		**	**	**	**	**	**	**	**	**	**	**	**	**	**	**
	26	*	0	17	26	41	53	69	84	91	99	110	112	112	112	**
	22	20	39	59	72	87	100	111	128	143	155	166	170	170	170	**
D	18	**	100	108	119	138	157	177	193	217	233	243	257	260	261	**
	14	**	**	170	175	189	213	260	293	320	348	380	408	418	420	**
	10	**	**	**	**	**	**	393	442	495	545	589	623	630	**	**
	8	**	**	**	**	**	**	550	569	628	680	729	770	**	**	**
		**	**	**	**	**	**	**	**	**	**	**	**	**	**	**
	26	*	0	32	47	65	99	116	113	105	99	96	93	67	0	**
	22	0	25	42	48	53	77	97	99	93	88	85	83	61	0	**
$\bar{V}$	18	**	0	25	37	40	53	72	81	79	75	72	70	52	0	**
	14	**	**	0	17	23	27	44	62	64	57	49	47	37	0	**
	10	**	**	**	**	**	**	0	38	47	38	23	9	0	**	**
	8	**	**	**	**	**	**	0	30	35	26	14	0	**	**	**
		**	**	**	**	**	**	**	**	**	**	**	**	**	**	**
	26	*	0	6	10	17	26	30	25	21	18	10	2	-3	0	**
	22	0	5	17	27	28	33	34	25	18	16	11	3	-2	0	**
$\bar{U}$	18	**	0	16	26	23	25	28	23	17	13	8	1	-2	0	**
	14	**	**	0	2	9	16	20	18	13	9	5	-2	-5	0	**
	10	**	**	**	**	**	**	0	8	5	4	1	-3	0	**	**
	8	**	**	**	**	**	**	0	3	-1	-1	1	0	**	**	**
		**	**	**	**	**	**	**	**	**	**	**	**	**	**	**

* Denotes isotherm rises to the surface to the East of this station
** Denotes solid boundary

TABLE IV - BASIC DATA FOR SECTION II

TABLE	Grid # → / Isotherms ↓	1	2	3	4	5	6	7	8	9	10	11	12	13	14	15
	26	5	10	15	20	25	30	35	45	55	65	75	80	83	87	90
	22	6	10	15	20	25	30	35	45	55	65	75	80	83	87	89
X	18	8	10	15	20	25	30	35	45	55	65	75	80	83	87	88
	14	9	10	15	20	25	30	35	45	55	65	75	80	83	87	**
	10	**	10	15	20	25	30	35	45	55	65	75	80	83	84	**
	8	**	12	15	20	25	30	35	45	55	65	75	80	81	**	**
		**	**	**	**	**	**	**	**	**	**	**	**	**	**	**
	26	0	22	40	51	62	70	78	86	90	90	90	90	90	90	90
	22	44	61	80	94	105	115	123	138	150	160	166	168	169	170	170
D	18	80	90	108	124	141	156	170	198	230	265	289	300	304	308	308
	14	103	110	140	167	191	218	240	290	337	384	421	446	458	470	**
	10	**	146	192	232	273	316	357	421	490	549	599	618	628	629	**
	8	**	250	281	333	376	412	447	510	580	661	728	752	756	**	**
		**	**	**	**	**	**	**	**	**	**	**	**	**	**	**
	26	0	80	116	131	139	142	140	134	124	105	84	69	57	37	0
	22	0	62	94	114	126	129	129	122	111	94	77	66	57	37	0
$\bar{V}$	18	0	49	78	99	111	113	113	107	94	78	63	53	47	32	0
	14	0	39	61	78	88	90	91	86	74	60	49	39	27	0	**
	10	**	0	26	43	49	52	57	58	49	38	30	24	17	0	**
	8	**	0	0	4	13	23	35	40	34	23	15	8	0	**	**
		**	**	**	**	**	**	**	**	**	**	**	**	**	**	**
	26	0	6	10	12	16	20	19	14	10	5	0	-7	-13	-13	0
	22	0	9	11	12	15	20	18	14	9	3	-4	-9	-14	-14	0
$\bar{U}$	18	0	11	12	11	14	17	16	12	6	-1	-7	-10	-15	-16	0
	14	0	11	12	10	12	15	14	11	5	-3	-8	-10	-8	0	**
	10	**	0	5	9	10	9	9	8	4	-1	-4	-6	-6	0	**
	8	**	0	3	6	6	3	4	5	3	3	3	0	0	**	**
		**	**	**	**	**	**	**	**	**	**	**	**	**	**	**

* Denotes isotherm rises to the surface to the East of this section.
** Denotes solid boundary

TABLE V - BASIC DATA FOR SECTION III

TABLE	Grid # → Isotherms ↓	1	2	3	4	5	6	7	8	9	10	11	12	13	14	15
	26	8	10	15	20	25	30	35	45	55	65	70	75	80	83	86
	22	8	10	15	20	25	30	35	45	55	65	70	75	80	83	85
X	18	9	10	15	20	25	30	35	45	55	65	70	75	80	83	84
	14	**	10	15	20	25	30	35	45	55	65	70	75	80	83	**
	10	**	10	15	20	25	30	35	45	55	65	70	75	79	**	**
	8	**	13	15	20	25	30	35	45	55	65	70	75	77	**	**
		**	**	**	**	**	**	**	**	**	**	**	**	**	**	**
	26	0	12	38	49	52	55	60	65	70	74	75	76	77	78	78
	22	46	60	81	90	92	94	96	106	120	135	140	142	146	147	147
D	18	80	83	100	109	120	133	151	180	210	239	251	262	271	278	279
	14	**	105	121	143	168	192	220	284	328	362	381	397	416	421	**
	10	**	135	171	203	234	284	323	397	461	527	555	586	610	**	**
	8	**	252	270	315	355	400	438	508	561	621	650	677	687	**	**
		**	**	**	**	**	**	**	**	**	**	**	**	**	**	**
	26	0	70	105	127	148	157	160	159	144	123	111	102	94	68	0
	22	0	49	85	112	130	138	137	131	124	115	108	101	94	68	0
$\bar{V}$	18	0	45	75	98	114	119	117	112	105	98	91	85	81	60	0
	14	**	0	55	83	90	87	81	79	79	78	71	63	44	0	**
	10	**	0	39	53	47	41	43	50	55	52	43	27	0	**	**
	8	**	0	9	12	12	12	17	29	39	38	29	17	0	**	**
		**	**	**	**	**	**	**	**	**	**	**	**	**	**	**
	26	0	2	3	5	8	11	12	11	11	10	8	7	8	7	0
	22	0	2	3	5	8	10	11	11	10	9	8	8	8	5	0
$\bar{U}$	18	0	2	3	4	5	8	10	9	6	3	5	7	6	2	0
	14	**	0	2	4	5	7	8	6	3	0	3	5	2	0	**
	10	**	0	2	3	3	4	5	3	1	0	2	3	0	**	**
	8	**	0	1	2	3	3	3	1	0	0	1	3	0	**	**
		**	**	**	**	**	**	**	**	**	**	**	**	**	**	**

* Denotes isotherm rises to the surface to the East of this station.
** Denotes solid boundary

TABLE VI - BASIC DATA FOR SECTION IV

TABLE	Grid # → Isotherms ↓	1	2	3	4	5	6	7	8	9	10	11	12	13	14	15
	26	*	34	35	40	45	50	55	65	75	85	95	105	115	**	**
	22	*	30	35	40	45	50	55	65	75	85	95	105	112	**	**
X	18	29	30	35	40	45	50	55	65	75	85	95	105	109	**	**
	14	**	**	36	40	45	50	55	65	75	85	95	105	**	**	**
	10	**	**	**	42	45	50	55	65	75	85	95	101	**	**	**
	8	**	**	**	**	48	50	55	65	75	85	92	**	**	**	**
		**	**	**	**	**	**	**	**	**	**	**	**	**	**	**
	26	*	0	11	50	80	99	107	120	125	127	130	131	134	**	**
	22	*	0	47	85	117	139	151	161	166	172	185	200	220	**	**
D	18	0	18	68	112	150	176	192	212	223	240	265	295	310	**	**
	14	**	**	110	140	173	212	243	284	323	355	380	405	**	**	**
	10	**	**	**	210	230	270	304	354	390	428	466	484	**	**	**
	8	**	**	**	**	310	325	359	430	497	567	615	**	**	**	**
		**	**	**	**	**	**	**	**	**	**	**	**	**	**	**
	26	0	0	61	93	109	128	147	146	136	123	98	59	0	**	**
	22	0	0	48	67	77	101	127	139	138	122	93	56	0	**	**
$\bar{V}$	18	0	17	33	42	52	75	102	122	127	111	85	53	0	**	**
	14	**	**	0	18	33	54	78	102	109	93	59	0	**	**	**
	10	**	**	**	0	9	27	51	81	92	81	54	0	**	**	**
	8	**	**	**	**	0	11	28	57	64	37	0	**	**	**	**
		**	**	**	**	**	**	**	**	**	**	**	**	**	**	**
	26	0	0	-3	-1	3	2	0	3	3	0	2	4	0	**	**
	22	0	0	-1	-1	2	0	-2	2	2	-2	1	4	0	**	**
$\bar{U}$	18	0	3	1	-1	1	-1	-3	1	0	-4	0	4	0	**	**
	14	**	**	0	-3	-1	-2	-3	1	-1	-5	-3	0	**	**	**
	10	**	**	**	0	2	-3	-1	3	1	-2	-1	0	**	**	**
	8	**	**	**	**	0	-5	2	4	2	1	0	**	**	**	**
		**	**	**	**	**	**	**	**	**	**	**	**	**	**	**

* Denotes isotherm rises to the surface to the East of this station
** Denotes solid boundary

Figure 4. Downstream Surface Current (V_s) vs Cross-Stream Distance with Envelope of Observed Variations - Sections I and II.

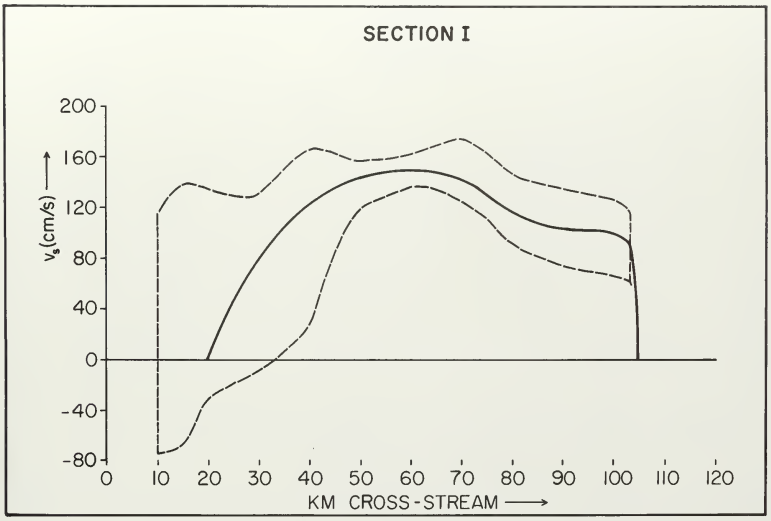
SECTION I
200
160
120
80
40
0
-40
-80
v_s (cm/s) ⟶
0 10 20 30 40 50 60 70 80 90 100 110 120
KM CROSS-STREAM ⟶

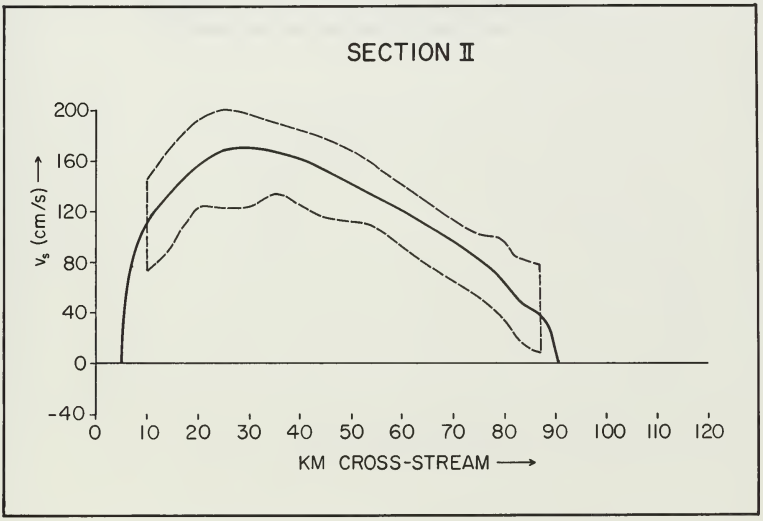
SECTION II
200
160
120
80
40
0
-40
v_s (cm/s) ⟶
0 10 20 30 40 50 60 70 80 90 100 110 120
KM CROSS-STREAM ⟶

Figure 5. Downstream Surface Current (V_s) vs Cross-Stream Distance with Envelope of Observed Variations - Sections III and IV.

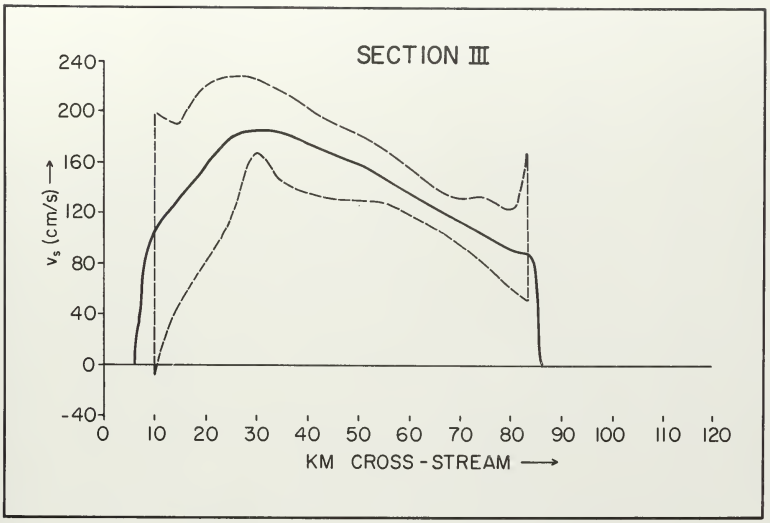
SECTION III
240
200
160
120
80
40
0
-40
v_s (cm/s) ⟶
0 10 20 30 40 50 60 70 80 90 100 110 120
KM CROSS-STREAM ⟶

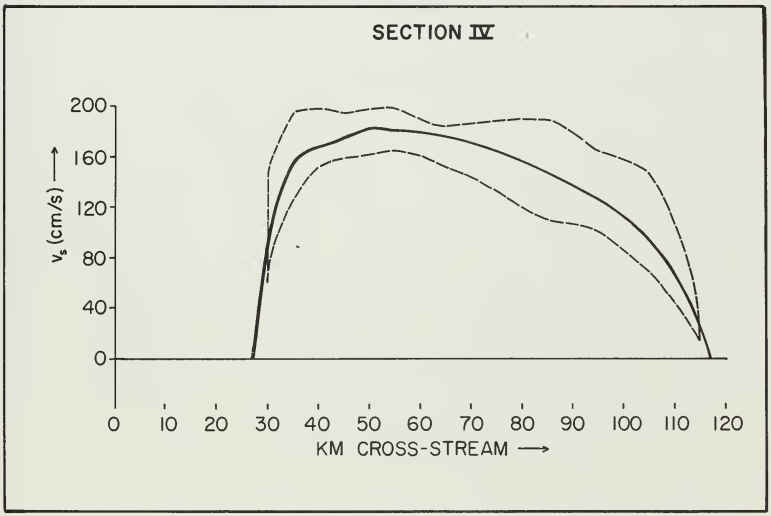
SECTION IV
200
160
120
80
40
0
v_s (cm/s) ⟶
0 10 20 30 40 50 60 70 80 90 100 110 120
KM CROSS-STREAM ⟶

Figure 6. Smoothed Downstream (V) Isotachs for Sections I and II.

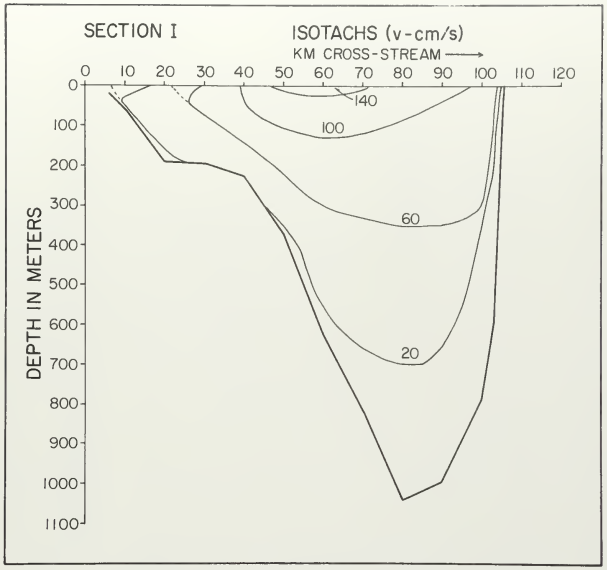
SECTION I
ISOTACHS (v-cm/s)
KM CROSS-STREAM
0 10 20 30 40 50 60 70 80 90 100 110 120
140
100
60
20
DEPTH IN METERS
0 100 200 300 400 500 600 700 800 900 1000 1100

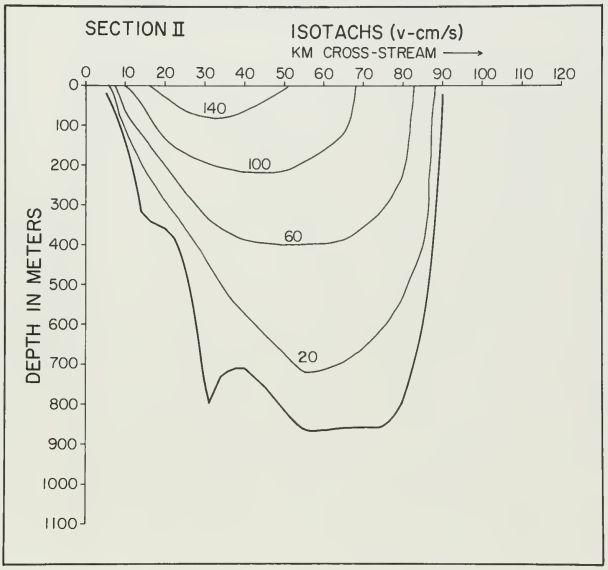
SECTION II
ISOTACHS (v-cm/s)
KM CROSS-STREAM
0 10 20 30 40 50 60 70 80 90 100 110 120
140
100
60
20
DEPTH IN METERS
0 100 200 300 400 500 600 700 800 900 1000 1100

Figure 7. Smoothed Downstream (V) Isotachs for Sections III and IV.

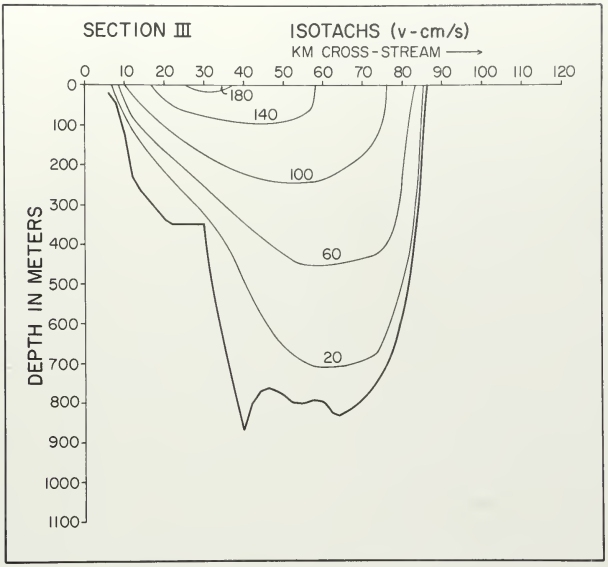
SECTION III
ISOTACHS (v-cm/s)
KM CROSS-STREAM →
0 10 20 30 40 50 60 70 80 90 100 110 120
180
140
100
60
20
DEPTH IN METERS
0 100 200 300 400 500 600 700 800 900 1000 1100

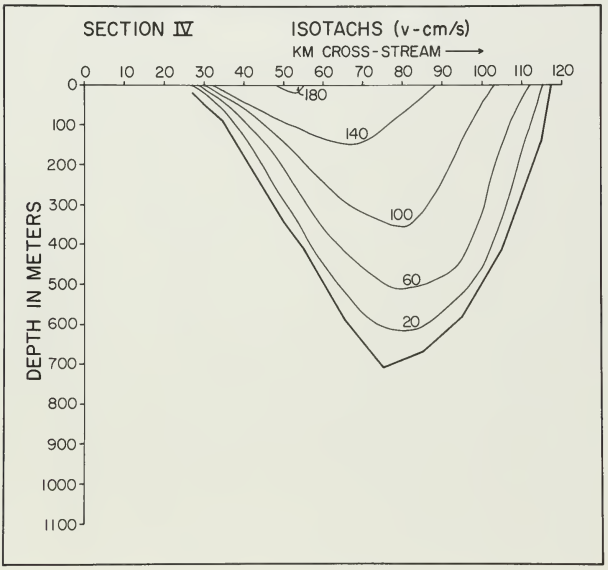
SECTION IV
ISOTACHS (v-cm/s)
KM CROSS-STREAM →
0 10 20 30 40 50 60 70 80 90 100 110 120
180
140
100
60
20
DEPTH IN METERS
0 100 200 300 400 500 600 700 800 900 1000 1100

Figure 8. Smoothed Cross-Stream (U) Isotachs for Sections I and II.

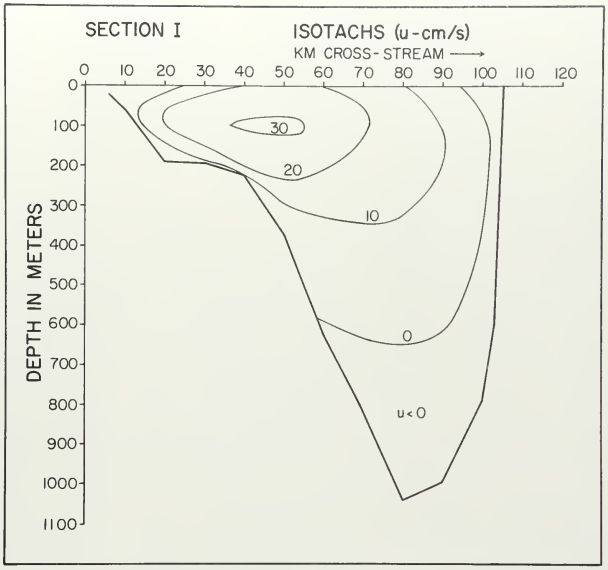
SECTION I
ISOTACHS (u-cm/s)
KM CROSS-STREAM
0 10 20 30 40 50 60 70 80 90 100 110 120
DEPTH IN METERS
0 100 200 300 400 500 600 700 800 900 1000 1100
30
20
10
0
u<0

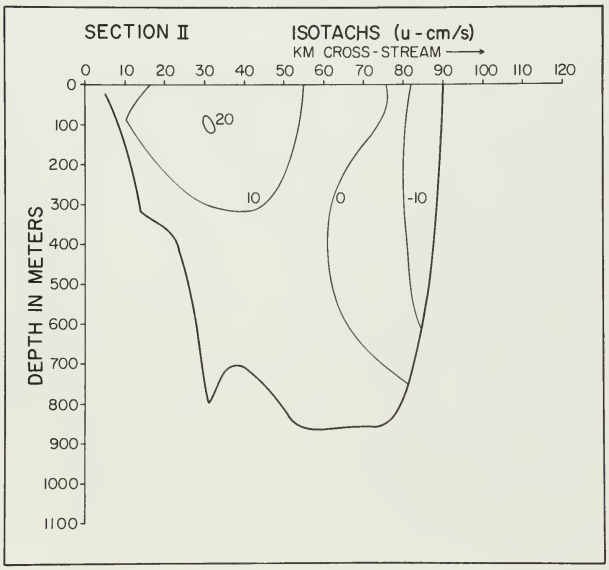
SECTION II
ISOTACHS (u-cm/s)
KM CROSS-STREAM
0 10 20 30 40 50 60 70 80 90 100 110 120
DEPTH IN METERS
0 100 200 300 400 500 600 700 800 900 1000 1100
20
10
0
-10

Figure 9. Smoothed Cross-Stream (U) Isotachs for Sections III and IV.

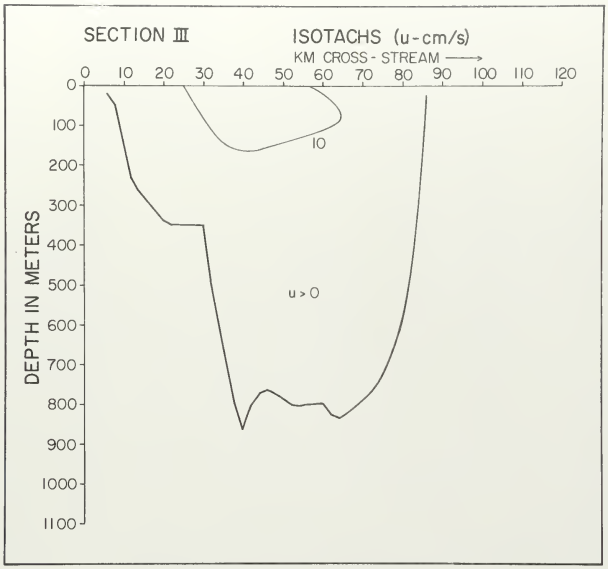
SECTION III
ISOTACHS (u-cm/s)
KM CROSS-STREAM
0 10 20 30 40 50 60 70 80 90 100 110 120
0 100 200 300 400 500 600 700 800 900 1000 1100
DEPTH IN METERS
10
u > 0

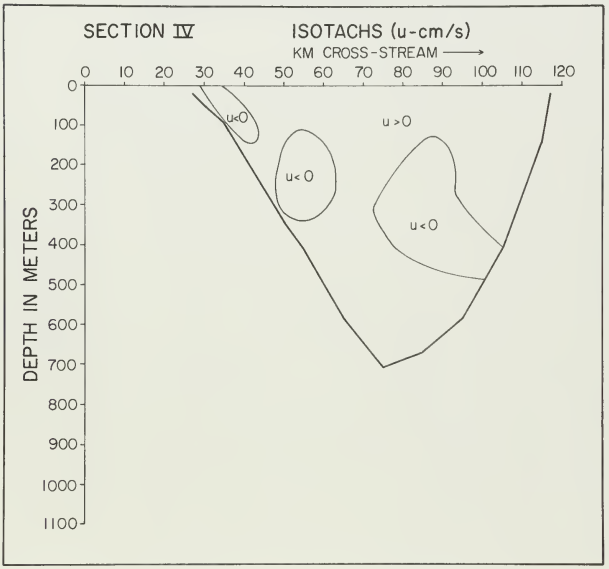
SECTION IV
ISOTACHS (u-cm/s)
KM CROSS-STREAM
0 10 20 30 40 50 60 70 80 90 100 110 120
0 100 200 300 400 500 600 700 800 900 1000 1100
DEPTH IN METERS
u<0
u > 0
u< 0
u<0

Figure 10. Isotherm Depths
for Sections I and II.

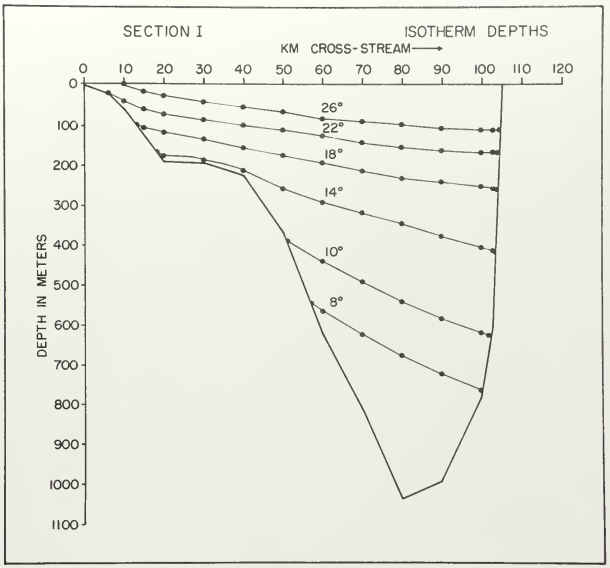
SECTION I
ISOTHERM DEPTHS
KM CROSS-STREAM
0 10 20 30 40 50 60 70 80 90 100 110 120
DEPTH IN METERS
0 100 200 300 400 500 600 700 800 900 1000 1100
26°
22°
18°
14°
10°
8°

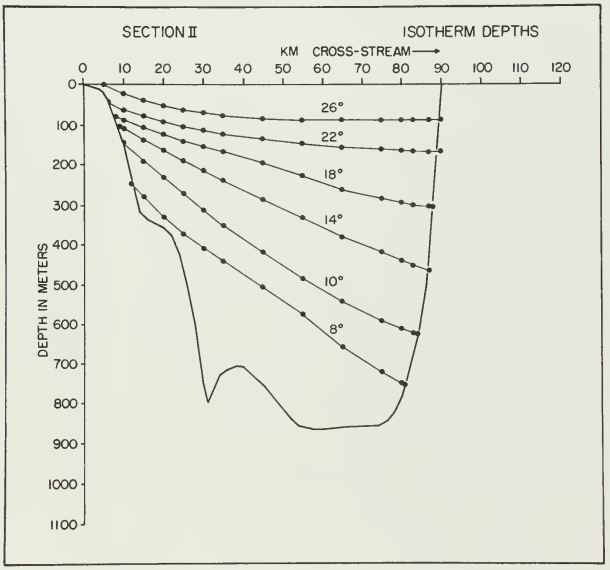
SECTION II
ISOTHERM DEPTHS
KM CROSS-STREAM
0 10 20 30 40 50 60 70 80 90 100 110 120
DEPTH IN METERS
0 100 200 300 400 500 600 700 800 900 1000 1100
26°
22°
18°
14°
10°
8°

Figure 11. Isotherm Depths
for Sections III and IV.

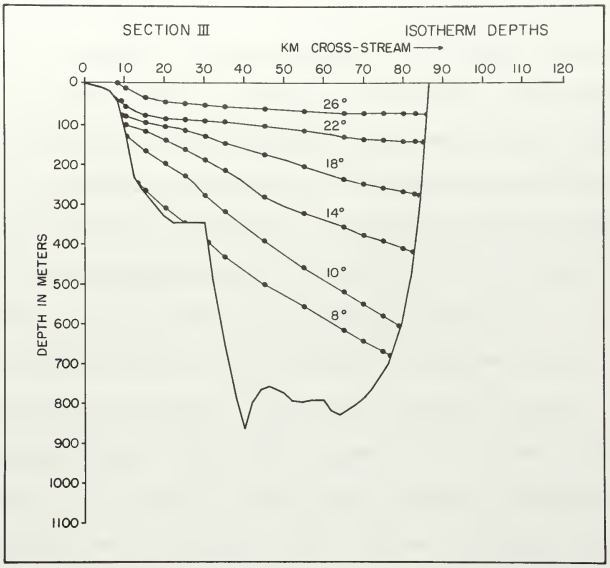
SECTION III
ISOTHERM DEPTHS
KM CROSS-STREAM
0 10 20 30 40 50 60 70 80 90 100 110 120
DEPTH IN METERS
0 100 200 300 400 500 600 700 800 900 1000 1100
26°
22°
18°
14°
10°
8°

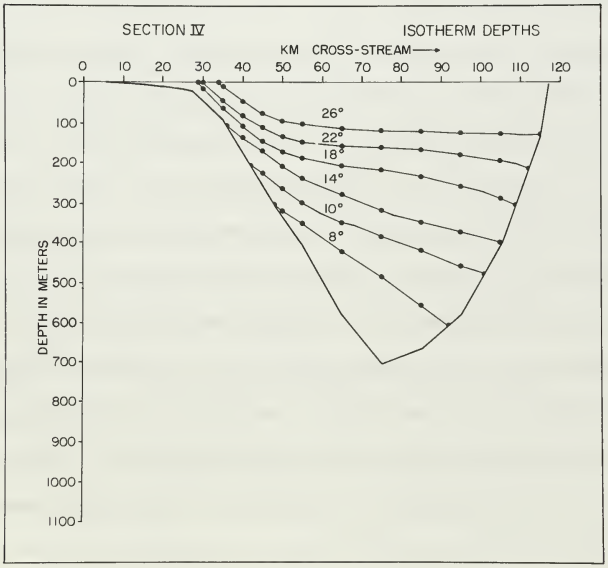
SECTION IV
ISOTHERM DEPTHS
KM CROSS-STREAM
0 10 20 30 40 50 60 70 80 90 100 110 120
DEPTH IN METERS
0 100 200 300 400 500 600 700 800 900 1000 1100
26°
22°
18°
14°
10°
8°

prior to opening onto the Blake Plateau. The eastern profile of the Straits maintains its characteristic steep slope in Sections I, II, and III with a reduced steepness in Section IV. The western slope of the Straits is more gradual, with a shelf at 200 m in Section I, deepening to about 300 m in Sections II and III, and losing its identity in Section IV. The average cross-sectional area of this 225 km downstream sector is about 50 km^2, the average depth about 600 m, and the width of the current is 80-100 km.

(2) Surface Current. With reference to Figures 4 and 5, the surface current is uniaxial. The surface current is fairly symmetric at Section I and clearly asymmetric to the west of center at Sections II, III, and IV. The surface current is characterized by a cyclonic zone to the west of the axis and an anticyclonic zone to the east, with thin layers of high shear at the channel boundaries. A typical value of the shear in the thin layer at the western boundary is 1 m/sec in 3-5 km. The shear in the cyclonic zone is about one-half of that value, decreasing to one-quarter of that value (and negative) in the anticyclonic zone. A typical value of the shear in the thin layer at the eastern boundary is 0.75 m/sec in 3-5 km.

Figures 4 and 5 show envelopes of fluctuation bounds (dotted lines) in the downstream surface current component (V_s) for each section, along with the mean profiles. The amplitude of the bounds are characteristically in the 20-30% range except at the current edges, particularly for Sections I and III and at the western edge of the current. The large bounds at the current edges are associated with a meandering motion. At Section I, the position of the edge of the current was observed to vary by 30 km, from X=5 to 35 km.

The mean position of the current edge was chosen at X=20 km and the "mean" profile brought to zero at that point. This large fluctuation in surface current on the western side of the channel is apparent in all four sections, although most pronounced in Section I and least pronounced in Section IV.

The symmetry of the surface current at Section I might be expected from the curvature effect as the east-bound current in the southern Straits begins its swing to the northeast. The current axis is found to the west of center as the channel converges at Section II. Between Sections II and III the curvature effect is small, but the channel further converges as the cross-stream distance at the surface is reduced by 4 km at the eastern boundary. The surface current remains asymmetric to the west of the channel center at Section IV.

The most important feature of the surface current is its downstream acceleration. The surface current accelerates downstream as the cross-channel width decreases between Section I and III and then decelerates slightly as the surface width diverges at Section IV.

(3) Subsurface Current. With reference to Figures 6 and 7, the subsurface current contours, like the surface current, show abrupt shear zones at both edges of the channel with characteristic regions of cyclonic and anticyclonic shear to the west and east of the axis, respectively. The cyclonic shear becomes more pronounced downstream.

The dominant feature of the current is a downstream acceleration. The higher velocity contours widen, deepen, and are displaced more to the west downstream, while the lower velocity contours tend to conform to the bottom topography of the area. As would be expected

from the continuity equation, the decrease in the cross-sectional area of the channel leads to the acceleration of the current. There is, however, a slight deceleration of the high speed layers between Sections III and IV as the cross-channel width increases at the surface.

As can be seen in Figures 8 and 9, the absolute value of cross-stream speed decreases downstream. There is a well-defined positive core at Section I, decreasing to Section III, and disappearing at Section IV. The change in cross-stream speeds between Sections I and II is associated with the curvature effect. The zones of negative cross-stream speeds at Sections I and II are associated with convergence on the east side of the channel, and the zone of positive cross-stream speed at the eastern side of the channel at Sections III and IV is associated with the diverging channel.

(4) Isotherm Distribution. The distribution of isotherms shows the cross-stream slope from west to east characteristic of Gulf Stream Regions, see Figures 10 and 11. On the average, the 8° and 10° isotherms always rise downstream. The upper isotherms also rise downstream except for the 22°, 18° and 14° isotherms, which lower between Sections I and II, and the 26°, 22° and 18° isotherms, which lower between Sections III and IV. The pattern of downstream changes in isotherm depths described above is associated with the downstream changes in the current field, and are qualitatively those anticipated from the Bernoulli Equation. Downstream changes along streamlines will not be discussed in this thesis.

B. Comparison with Other Methods

Free instrument data will be compared with (1) current meter measurements (2) GEK surface current measurements, and (3) hydrographic data. The comparison with these methods is shown in Figures 12-15. In all figures, the dotted lines show free instrument results and solid lines the compared data.

(1) Pillsbury (1890) made over 1,100 hours of direct current measurements during 1885-1886. Using an anchored current meter of his own design, current measurements were made at depths of 6, 27, 55, 119, and 238 m at each of six anchor stations between Fowey Rocks and Gun Cay, B.W.I. Current measurements to a depth of 370 m were made at the easternmost station. Pillsbury assumed a linear decrease in velocity with depth below the depth of his measurements. Therefore, his description of the deep current structure was based on this extrapolation from his measured values, and resulted in a contour of zero velocity above the bottom. Below this zero velocity contour he concluded that the current was either at rest or setting southward. He also reported a uniaxial surface current with a displacement of the axis to the west of channel center.

A comparison of free instrument data at Section II with that of Pillsbury's is shown in Figure 12. It should be noted that Pillsbury's data was taken 8.4 km downstream of this section. However, the correlation in surface current is good, with the only meaningful deviation being near the western boundary. This is probably due to his linear extrapolation from the 14 km distance of his westernmost station to the point of zero velocity. Pillsbury's subsurface speed contours, with the exception of his zero velocity

Figure 12. Comparison of Free Instrument Surface and Subsurface Current Data at Section II with Current Meter Data.

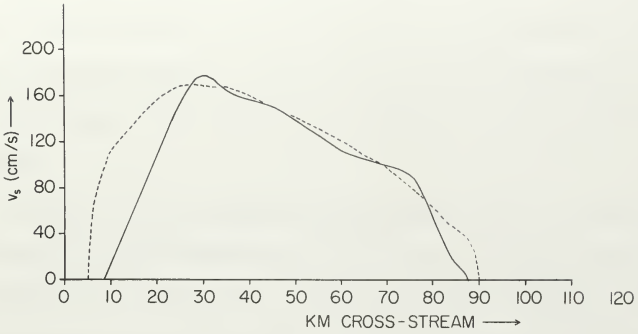
200
160
120
80
40
0
v_s (cm/s) ⟶
0 10 20 30 40 50 60 70 80 90 100 110 120
KM CROSS-STREAM ⟶

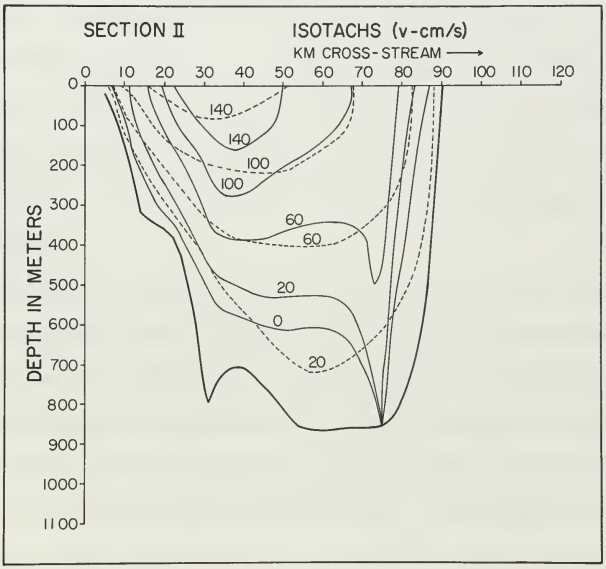
SECTION II
ISOTACHS (v-cm/s)
KM CROSS-STREAM ⟶
0 10 20 30 40 50 60 70 80 90 100 110 120
DEPTH IN METERS
0
100
200
300
400
500
600
700
800
900
1000
1100
140
140
100
100
60
60
20
0
20

contour and those contours constructed from extrapolated values, compare favorably with our results. However, there are measurable differences in the depths of the high speed contours. Considering the fact that there were over twice as many free instrument stations as current meter stations (in particular note the differences on the western edge of the current), the contours are quite similar in shape.

(2) Webster (1961) computed time-averaged surface currents on the basis of 632 GEK measurements made during 42 cruises between Fowey Rocks and Gun Cay, B.W.I., during the period 1952-1958. These cruises were made by the Institute of Marine Science of the University of Miami, for example see Anon, 1954. Webster divided the current into eleven zones of 5-8 km each, and averaged the surface velocity components in each zone. A comparison of the average surface current resulting from these measurements with the free instrument surface current profile at Section II is shown in Figure 13a. Current velocity is brought to zero at boundaries coincident with those at Section II for ease of comparison. In general, the comparison shows a remarkable similarity, the only exception being an increased speed at the current axis.

In contrast to time-averaged data, Figure 13b shows a comparison of free instrument data at Section III with a single uncorrected GEK transect (Murray, 1952) taken on May 26, 1951. The multiaxial current structure shown from this GEK data is seldom observed on a single transect with the free instrument technique, and is certainly not a feature of the steady state Florida Current. A multiaxial current structure is often reported from data obtained along a single transect

Figure 13. Comparison of Free Instrument Surface Current Data at Sections I and II with GEK Data. (a) Webster (1961)
(b) Murray (1952)
(c) Chew and Wagner (1956)

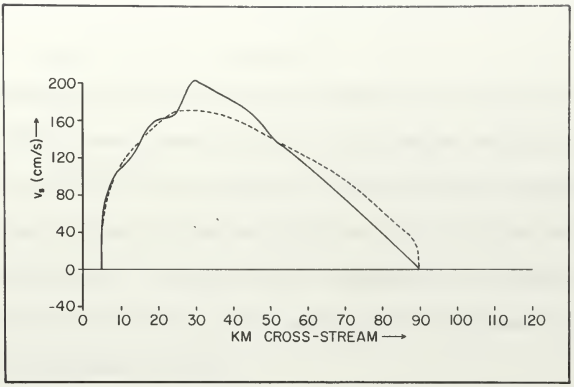
200
160
120
80
40
0
-40
v_s (cm/s) ⟶
0 10 20 30 40 50 60 70 80 90 100 110 120
KM CROSS-STREAM ⟶

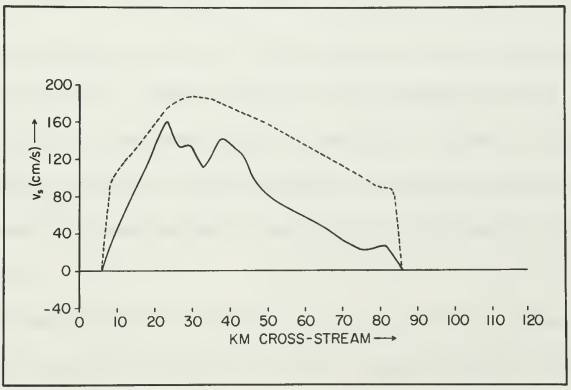
200
160
120
80
40
0
-40
v_s (cm/s) ⟶
0 10 20 30 40 50 60 70 80 90 100 110 120
KM CROSS-STREAM ⟶

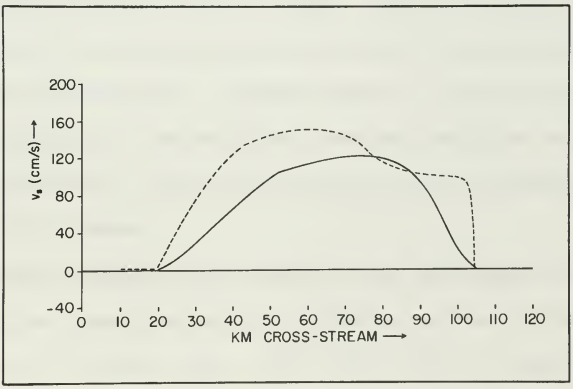
200
160
120
80
40
0
-40
v_s (cm/s) ⟶
0 10 20 30 40 50 60 70 80 90 100 110 120
KM CROSS-STREAM ⟶

across the current, where the time scale of crossing is greater than six hours, suggesting tidal aliasing.

A comparison of free instrument surface current data at Section I is made with GEK measurements taken in this region during a single transect in July 1953, see Figure 13c. The corrected measurements were smoothed by Chew and Wagner (1956) as their interpretation of time-averaged data. Although there is agreement in absolute values and symmetry of the curves, the current axis is displaced to the east of the free instrument results.

(3) The same cruise report (Chew and Wagner, 1956) listed isotherm depths from a series of hydrographic stations completed on August 25, 1955. Figure 14a shows these isotherm depths as they compare with free instrument data at Section I. There is agreement in the general symmetry of the isotherms, although the hydrographic results show the characteristic undulations attributable to tidally biased data.

Worthington (1966) has kindly made available data taken from hydrographic stations during an Atlantis cruise in the Ft. Pierce-Matanilla Shoal region on June 25, 1955. Figure 14b shows a comparison of this data with the isotherm depths from free instrument measurements at Section IV. Although there is a favorable correlation in shape and slope of the isotherms, there are variations in their vertical separation, again possibly showing a tidal influence on data from a single transect.

In marked contrast to non-synoptic data, the averaged temperature data from four summer hydrographic cruises across the Florida Current near Section II (Broida, 1962a, 1962b, 1963, 1964) is compared with

results of the free instrument method. Figure 15a shows a comparison of this time-averaged data and is in good agreement with the results of our experiment. Figure 15b shows the fluctuations in the 26°, 18°, and 8° isotherms over the four cruises. These same isotherms from free instrument data fall within the envelope of the variations.

Figure 14. Comparison of Free Instrument Mass Field Data at Sections I and IV with Hydrographic Data. (a) Chew and Wagner (1956) (b) Worthington (1966)

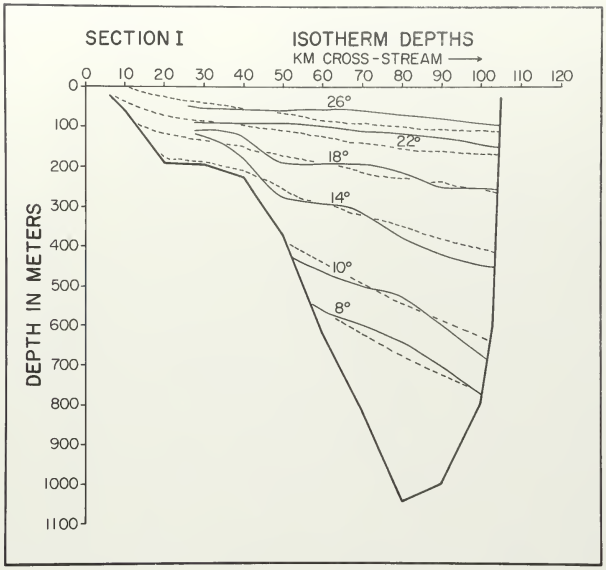
SECTION I
ISOTHERM DEPTHS
KM CROSS-STREAM →
0 10 20 30 40 50 60 70 80 90 100 110 120
DEPTH IN METERS
0 100 200 300 400 500 600 700 800 900 1000 1100
26°
22°
18°
14°
10°
8°

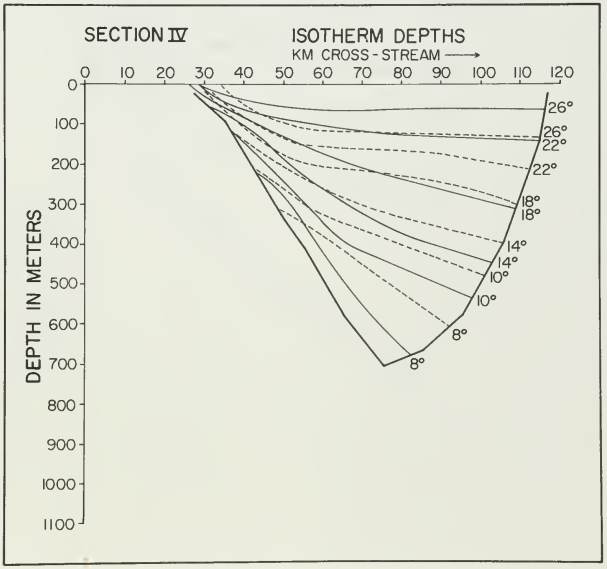
SECTION IV
ISOTHERM DEPTHS
KM CROSS-STREAM →
0 10 20 30 40 50 60 70 80 90 100 110 120
DEPTH IN METERS
0 100 200 300 400 500 600 700 800 900 1000 1100
26°
26°
22°
22°
18°
18°
14°
14°
10°
10°
8°
8°

Figure 15. Comparison of Free Instrument Mass Field Data at Section II with Time-Averaged Hydrographic Data.
(a) Comparison of Data
(b) Variations in Hydrographic Data

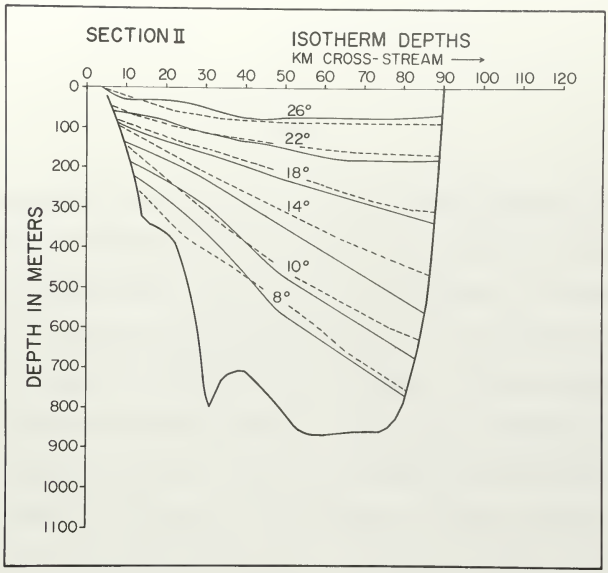
SECTION II
ISOTHERM DEPTHS
KM CROSS-STREAM →
0 10 20 30 40 50 60 70 80 90 100 110 120
0 100 200 300 400 500 600 700 800 900 1000 1100
DEPTH IN METERS
26°
22°
18°
14°
10°
8°

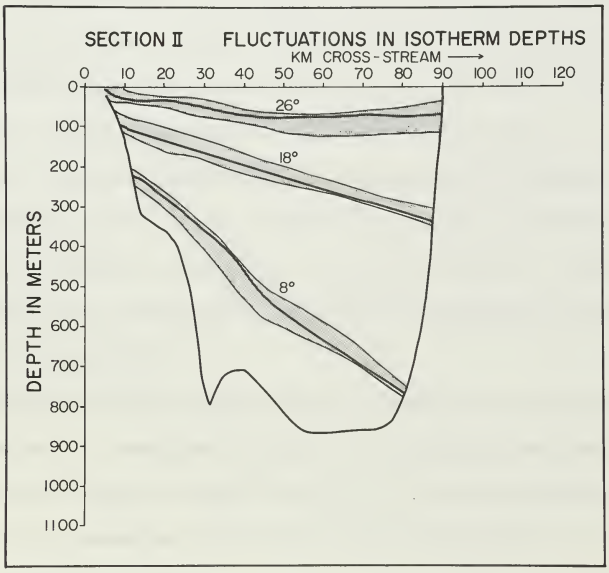
SECTION II
FLUCTUATIONS IN ISOTHERM DEPTHS
KM CROSS-STREAM →
0 10 20 30 40 50 60 70 80 90 100 110 120
0 100 200 300 400 500 600 700 800 900 1000 1100
DEPTH IN METERS
26°
18°
8°

IV. SUMMARY

Characteristic features of the velocity and temperature fields in the Florida Current have been isolated and discussed on the basis of free instrument data obtained during approximately 40 transects across the current at four separate sections. The data was obtained during the summers of 1965-1966 and encompasses a 225 km downstream distance within the Florida Straits. Each transect consisted of about 10 stations, and each station was sampled several times in a serious effort to average over fluctuations in order to obtain a coherent representation of the mean or steady state mass and velocity fields. The experiment was designed to provide data for testing models of the current dynamics. The results have been presented in x,y,T (cross-stream, downstream, temperature) coordinates at six temperature levels since data in this form are convenient to the testing of three-dimensional inertial current models (Robinson, 1965). As a first step, this thesis presents a description of the dominant features of the mass (temperature) and velocity fields. Also, the data obtained has been compared with previous observations in the area of the experiment.

The most important original result obtained is the determination of the nature of downstream responses of the mass and velocity fields to downstream changes in channel geometry. The most significant result of the comparison with previous time-averaged data is the general agreement obtained.

The major conclusions are:

(1) The surface current is uniaxial, symmetrical about the current center at Section I due to the curvature effect and asymmetric to the west of current center as the channel converges at Sections II-IV. The surface current accelerates between Sections I and III and decelerates slightly at Section IV, clearly associated with changes in channel width.

(2) The downstream subsurface current retains the shape of the surface current. Between Sections I and II there is a strong (30%) acceleration in the upper layers, which penetrates in depth between Sections II-IV. As would be expected from the continuity equation, this phenomenon is associated with changes in cross-sectional area of the channel.

(3) Cross-stream current fields near the channel boundaries are primarily associated with the converging and diverging topography, while absolute values of cross-stream speed decrease downstream as the curvature effect decreases.

(4) Isotherms rise downstream where the current is accelerated and lower where the current is decelerated, in agreement with Bernoulli's Equation.

(5) The comparison of the free instrument method with Pillsbury's current meter data and GEK and hydrographic data shows close agreement where time-averaged data is the basis for comparison.

LITERATURE CITED

Anon, 1954. Some results of the Florida Current Study, 1953. Inst. Mar. Sci. Univ. of Miami, Tech. Rept. No. 54-7. Unpublished manuscript.

Broida, Saul, 1962a. A report of data obtained in Florida Straits and off the West Coast of Florida. January-June 1961. Inst. Mar. Sci. Univ. of Miami, No. 62-4. Unpublished manuscript.

1962b. A report of data obtained in Florida Straits and off the West Coast of Florida. January-June 1962. Inst. Mar. Sci. Univ. of Miami, No. 62-11. Unpublished manuscript.

1963. A report of data obtained in Florida Straits and off the West Coast of Florida. July-December 1962. Inst. Mar. Sci. Univ. of Miami, No. 63-3. Unpublished manuscript.

1964. A report of data obtained in Florida Straits and off the West Coast of Florida. January-June 1963. Inst. Mar. Sci. Univ. of Miami, No. 64-1. Unpublished manuscript.

Chew, Frank and Wagner, L. P., 1956. Semi-Annual report of investigation between the period of 15 May 1955 to 15 November 1955. Univ. of Miami Mar. Lab. Semi-Annual Rept. No. 56-15.

Murray, K. M., 1952. Short period fluctuations of the Florida Current from geomagnetic electrokinetograph observations. Bull. Mar. Sci. Gulf and Carib., 2, pp. 360-375.

Pillsbury, J. E., 1890. The Gulf Stream - a description of the methods employed in the investigation, and the results of the research. Rept. Supt., U. S. Coast Geod. Surv., Appendix 10, pp. 461-620.

Richardson, W. S. and Schmitz, W. J. Jr., 1965. A technique for the direct measurement of transport with application to the Straits of Florida. Jour. Mar. Res., 23, pp. 172-185.

Robinson, A. R., 1965. A three-dimensional model of inertial currents in a variable-density ocean. Jour. Fluid Mech. 21, pp. 211-223.

Schmitz, W. J. Jr., 1966. On the dynamics of the Florida Current. Doctoral Dissertation. University of Miami.

Schmitz, W. J. Jr. and Richardson, W. S., 1966. A preliminary report on Operation Strait Jacket. Univ. of Miami Inst. Mar. Sci. Tech. Rept. (Unpublished manuscript).

Webster, Ferris, 1961. The effects of meanders on the kinetic energy balance of the Gulf Stream. Tellus, 13, pp. 392-401.

Worthington, L. V., 1966. Unpublished data from Atlantis cruise, June 1955. (Personal communication).

VITA

CDR Edward Clausner, Jr., USN, was born in Buffalo, New York, on October 27, 1929. His parents are Maurice Edward Clausner and Lucille Emily Clausner. He received his elementary education at South Mountain School, Millburn, New Jersey, and his secondary education at Millburn High School, Millburn, New Jersey.

In August 1947 he entered the U.S. Naval Academy, Annapolis, Maryland. Upon graduating in June 1951 with a B.S., he was commissioned an Ensign in the U.S. Navy. Subsequent naval service included one and one half years of service in amphibious force ships of the Pacific Fleet, followed by twelve years of submarine service in the Atlantic Fleet. He attended the U.S. Naval War College, Newport, Rhode Island during 1962-1963 prior to two years of service as Commanding Officer of USS TIRANTE (SS420).

He was admitted to the Graduate School of the University of Miami in September 1965. He was granted the degree of Master of Science in June 1967.

Permanent address: 1444 S.E. 15th Court
Deerfield Beach, Florida

thesC505
Characteristic features of the Florida C
3 2768 002 10293 1
DUDLEY KNOX LIBRARY